1.6 ARCTIC OCEAN/SEA-ICE RESPONSE TO CLIMATE VARIABILITY IN A COUPLED MODEL

Xiangdong Zhang *
University of Alaska Fairbanks, AK99775, USA

Moto Ikeda
Hokkaido University, Sapporo 060-0810, Japan

1. Introduction

Recent studies demonstrated that the Arctic climate is undergoing remarkable changes. A much weaker Beaufort high and a sharp increase in cyclonic activity have happened over the central Arctic Ocean since 1988 (Walsh et al., 1996). Long-term sea level pressure records show a leading dynamic annular mode, the Arctic Oscillation (AO), as recognized by Thompson and Wallace (1998). They also showed that the AO trend is close associated with surface air temperature increase. With the satellite passive-microwave data, Parkinson et al. (1999) indicated an overall decreasing trend of 2.8% in the Arctic sea-ice extents. Submarine measurements also show the mean sea-ice thickness decreased by 1.3m between the period 1958-1976 and 1993-1997 (Rothrock et al., 1999). Moreover, the comparison of Ocean hydrographic data in 1990s reveals that the Eurasian Basin "cold halocline layer" has retreated from the Amundsen Basin back into the Makarov Basin (Steele and Boyd, 1998). Thinning and lessening of sea-ice, retreating of halocline and warming of ocean may attribute to AO and global warming. In terms of the lack of observations in the Arctic Ocean, numerical model is a good tool to explore sea-ice and ocean changes and variations.

2. Model and Forcing Data

We employed a coupled Arctic ocean/sea-ice model, which was further developed for climate studies by Zhang and Zhang (2001). The ocean model is based on GFDL MOM2.0 (Pacanowski, 1995) and characterized by the flux-corrected-transport (FCT) algorithm (Gerdes et al., 1991), which is used to assure the pathway and properties of Atlantic water. The sea-ice model follows Hibler (1979) dynamics and Parkinson and Washington (1979) thermodynamics with modifications after Oberhuber et al. (1993) and (Fichefet and Maqueda, 1997). A simple parameterization of brine rejection and more sophisticated parameterizations of heat and freshwater are implemented (Zhang and Zhang, 1999). We developed a synchronous coupling scheme between ocean and sea-ice to help energy and freshwater conserved. For details, see Zhang and Zhang (2001).

The forcing data is constructed from NCEP/NCAR reanalysis data for 1958 through 1998 (Kalnay et al., 1996). They include surface windstress, 2m air temperature, 2m specific humidity, surface pressure. Downwelling shortwave and longwave radiation are calculated by parameterization schemes preferred for Arctic region (Key et al., 1996; Zhang and Zhang, 2001). Precipitation and river runoff are taken from climate observations (Legates and Willmott, 1990; NSIDC; Becker, 1995).

3. Results

3.1 Leading Mode of Climate Variability Over the Arctic

Thompson and Wallace (1998) made an empirical orthogonal function (EOF) diagnosis on the monthly mean sea level pressure (SLP) north of $20^{o}N$ and recognized the annular mode with action center focusing on the Arctic Ocean domain. In order to concentrate to the Arctic Ocean, we make an EOF analysis on the SLP north of $62.5^{o}N$ to represent the Arctic dominant mode of climate variability. In terms of convergence of meridian, area-weighting is applied in EOF diagnosis. The spatial pattern of the leading mode is pretty similar to the AO pattern, with the action center located near the Spitsbergen. The time series of first principle component shows that SLP is getting lower over the Arctic Ocean since late 1980s, the same as AO. Similar to AO, we define the lower SLP episode as the positive phase of climate variability.

* *Corresponding author address:* Xiangdong Zhang, Frontier Research System for Global Change, International Arctic Research Center, University of Alaska Fairbanks, Fairbanks, AK99775; email: xdz@iarc.uaf.edu.

We made regression analyses of our forcing data on the first principle component corresponding to the positive and negative phase of leading SLP mode. These regressed variables are adopted as anomalies applied to our modeling experiments. Figure 1 shows the difference of 2m air temperature and windstress between the positive phase and negative phase. The cyclonic tendency of windstress is prevailing over the whole arctic domain. The positive air temperature anomaly occupies the Arctic Ocean except the Bering Strait, the Canadian Archipelago and part of the GIN Sea. The highest temperature anomaly occurs from the Barents Sea to the Laptev Sea.

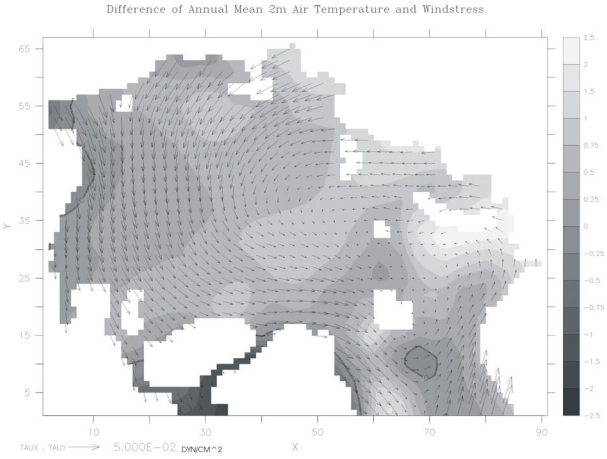

Fig.1 Difference of 2m air temperature (^{o}C) and windstress (dyn/cm^{2}) between the positive and negative phases of leading SLP mode.

3.2 Changes of Sea-ice and Hydrographic Properties

To explore the changes of the Arctic Ocean corresponding to the leading SLP mode, we performed two parallel modeling experiments with the forcing data constructed by addition of long-term climate mean and the anomalies corresponding to the positive and negative phases of the leading mode. Each experiment is carried out for ten years.

Figure 2 displays the difference of sea-ice concentration and velocities between two experiments. Consistent with the positive phase of the leading mode, sea-ice movement shows a cyclonic pattern, reverse to the climate mean. Sea-ice areas are much decreased in the sea-ice marginal zones, for example, the Barents Sea, the Laptev Sea, the Chukchi Sea and the Beaufort Sea. But sea-ice concentration increases off the Canadian Archipelago, caused by anomaly sea-ice movement, which is favorable to push sea-ice towards that region. Overall, the simulated results is quite close to the recent diagnostic ones regressed on AO by Rigor et al. (2001). Model shows more detailed information with accumulation of sea-ice in the Kara Sea resulting from sea-ice dynamics. A major lose of sea-ice concentration in the East Siberian Sea is not captured by model, compared with observation studies.

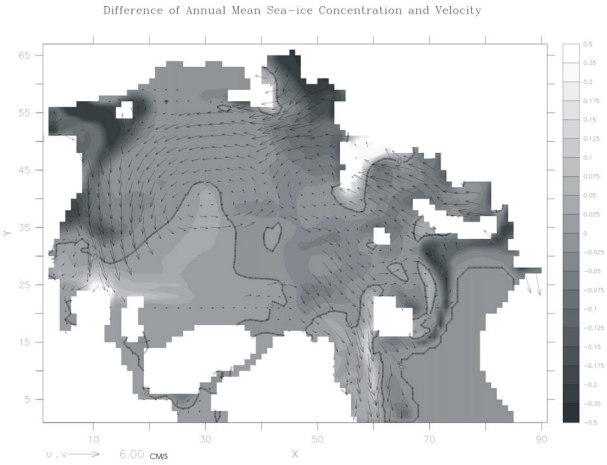

Fig.2 The same as figure 1 but for sea-ice concentration and velocity (cm/s).

On the other respect, sea-ice thickness may reflect more accurate changes. As shown in Figure 3, the predominant decrease of sea-ice thickness happens in the East Siberian Sea. It can reach about $2m$. Also it is clear to see the sea-ice piles up off the Canadian Archipelago with maximum value arriving at $3m$.

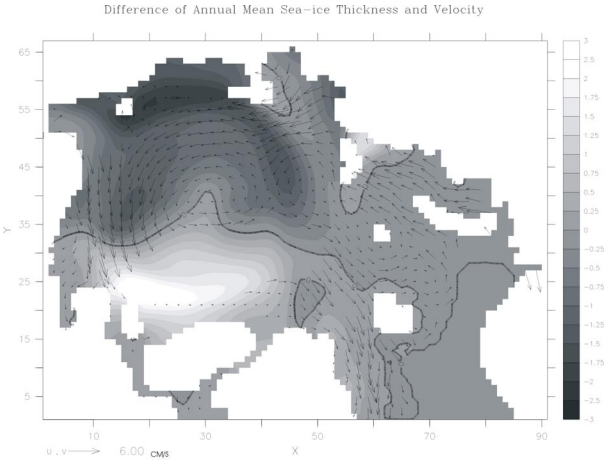

Fig.3 The same as figure 1 but for sea-ice thickness (m) and velocity (cm/s).

In terms of figure 2 and 3, sea-ice is overall decreased, responding to the positive phase of the leading mode and accompanying air temperature rising. However, sea-ice can be increased in some areas by the interplay of its thermodynamics and dynamics. Sea-ice motion plays an important role in the positive anomaly of sea-ice thickness.

Moreover, the ocean part is also changes a lot with the atmosphere variability. Figure 3 depicts the difference of heat content and vertical averaged velocity within the upper $\mathbf{210}\boldsymbol{m}$ of the Arctic Ocean, showing anomalous oceanic circulations and thermodynamic properties. Anomalous cyclonic circulation is dominant in the upper Arctic Ocean domain and the Arctic Ocean gets more heat, implying warmer ocean water. The flow from the GIN Sea through the Barents Sea to the Eurasian Basin is stronger. The largest heat content appears in the Barents Sea but it seems not caused by strengthened ocean flow. The Beaufort Gyre gets weakened because of cyclonic circulation anomaly over there.

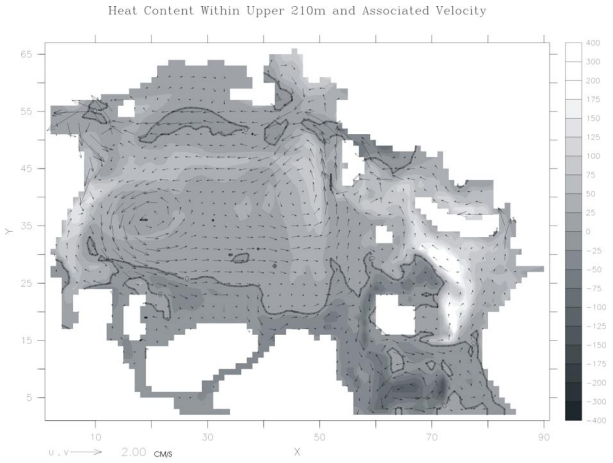

Fig. 4 The same as figure 1 but for heat content ($^{o}\boldsymbol{Cm}$) and vertical averaged velocity ($\boldsymbol{cm}/\boldsymbol{s}$) within the upper $\mathbf{210}\boldsymbol{m}$.

Another interesting phenomenon is an anomalous cyclonic circulation in the eastern Eurasian Basin with a local positive heat content anomaly. Through Fram Strait, the Atlantic flow is weaker than climate average and seems more Arctic cold water goes out to the GIN Sea and gives rise to a negative heat content anomaly there.

The Arctic freshwater budget has been paid much attention because of its potential effects on the thermohaline circulation and multi-decadal climate variability (Dickson, et al., 1988; Aagaard and Carmack, 1989; Griffies and Bryan, 1997). Figure 5 shows the difference of freshwater storage anomalies. In the positive phase of the leading SLP mode, more freshwater are accumulated on the side of North America from the Beaufort Sea and the Canada Basin off Canadian Archipelago to the Greenland Sea. Meanwhile, we could also infer from the figure 5 that more Arctic cold freshwater flows out of the Arctic Ocean via Fram Strait and causes the GIN Sea fresher. This could be influencing deep convections over there.

The freshwater storage in the Eurasian Basin and the Canada Basin is in deficiency. Together with the above heat content figure, the Eurasian Basin is getting warmer and saltier during the positive phase of the leading SLP mode. The modeling results are consistent with what Steele and Boyd (1998) have found that the "cold halocline layer" has retreated from the Amundsen Basin back into the Makarov Basin.

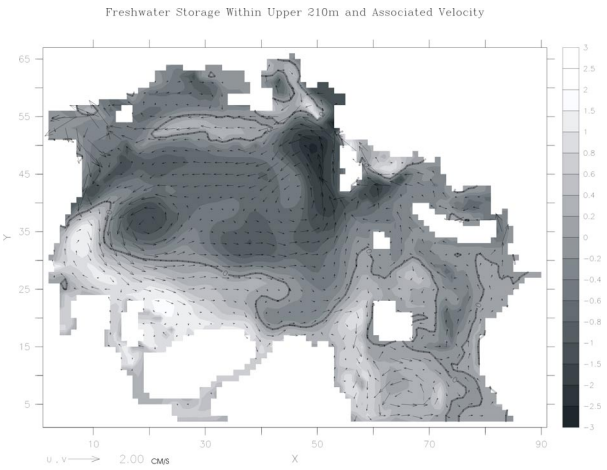

Fig. 5 The same as figure 1 but for freshwater storage ($\boldsymbol{m}$) and vertical averaged velocity ($\boldsymbol{cm}/\boldsymbol{s}$).

4. Concluding Remarks

We employed a coupled Arctic ocean/sea-ice model to explore the response of sea-ice and ocean to the leading mode of climate variability. The differences between positive and negative phases of leading SLP mode show a dramatic changes in sea-ice and ocean hydrographic features.

Since late 1980s, positive phase of AO or the leading mode used in this paper persists. This dominant climate variability mode contribute to the recent findings of overall decreasing of sea-ice, warming of ocean water and retreating of cold halocline. In the regime of positive phase of the leading mode, the GIN Sea and the Canadian

Archipelago are characterized by colder and fresher water, which seems like a manifestation of GSA (Great Salinity Anomaly) phenomenon. In addition, model indicates accumulation of sea-ice and freshwater storage on the side of northern American continent, which also attribute to the atmospheric circulations.

5. Reference

Aagaard, K., and E. C. Carmack, 1989: The role of sea ice and other fresh water in the Arctic circulation, *J. Geophys. Res., 94*, 14,485-14,497.

Dickson, R.R., J. Meinke, S. A. Malmberg, and A. J. Lee, The "Great Salinity Anomaly" in the northern North Atlantic 1968-1982, *Progress in Oceanography, 20*, 103-151, 1988.

Fichefet, T., and M. A. M. Maqueda, 1997: Sensitivity of a global sea ice model to the treatment of ice thermodynamics and dynamics. *J. Geophys. Res., 102,* 12,609-12,646.

Griffies, S. M., and K. Bryan, 1997: A predictability study of simulated North Atlantic multidecadal variability, *Clim. Dyn., 13*, 459-487.

Pacanowski, R. C., 1995: MOM2 user's guide and reference manual, *GFDL Ocean Group Tech. Rep.* 3, 232pp., NOAA Geophys. Fuid Dyn. Lab., Princeton, N. J.

Parkinson, C. L., D. J. Cavalieri, P. Gloersen, H. J. Zwally, and J. C. Comiso, 1999: Arctic sea ice extents, areas, and trends, 1978-1996. *J. Geophys. Res., 104*, 20,837-20,856.

Rigor, I. G., J. M. Wallace, and R. L. Colony, 2001: On the response of sea ice to the Arctic Oscillation. Submitted to *J. Clim.*

Rothrock, D. A., Y. Yu, and G. A. Maykut, 1999: Thinning of the arctic sea ice cover, *Geophys. Res. Lett., 26,* 3469-3472.

Steele, M., and T. Boyd, 1998: Retreat of the cold halocline layer in the Arctic Ocean. *J. Geophys. Res., 103,* 10,419-10,435.

Thompson, D. W., and J. M. Wallace, 1998: The Arctic Oscillation signature in the winter time geopotential height and temperature fields, *Geophys. Res. Lett.*, 25, 1297-1300.

Walsh, J. E., W. L. Chapman, and T. L. Shy, 1996: Recent decrease of sea level pressure in the central Arctic, *J. Clim.*, 9, 480-486.

Zhang, X., and J. Zhang, 2001: Heat and freshwater budgets and their pathways in the Arctic Mediterranean, *J. Oceanogr. 57,* 207-234.